Considerations for the acquisition and inversion of NMR T2 data in shales

Article *in* Journal of Petroleum Science and Engineering · November 2018

DOI: 10.1016/j.petrol.2018.10.109

2 authors:

Nadia Testamanti
Curtin University
11 PUBLICATIONS **20** CITATIONS
SEE PROFILE

Reza Rezaee
Curtin University
186 PUBLICATIONS **1,477** CITATIONS
SEE PROFILE

Accepted Manuscript

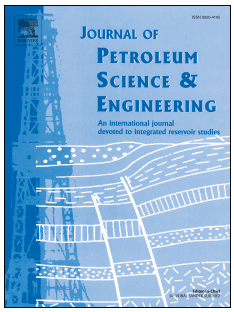

Considerations for the acquisition and inversion of NMR T_2 data in shales

M. Nadia Testamanti, Reza Rezaee

PII: S0920-4105(18)30977-X

DOI: https://doi.org/10.1016/j.petrol.2018.10.109

Reference: PETROL 5472

To appear in: *Journal of Petroleum Science and Engineering*

Received Date: 29 May 2018

Revised Date: 26 October 2018

Accepted Date: 30 October 2018

Please cite this article as: Testamanti, M.N., Rezaee, R., Considerations for the acquisition and inversion of NMR T_2 data in shales, *Journal of Petroleum Science and Engineering* (2018), doi: https://doi.org/10.1016/j.petrol.2018.10.109.

Considerations for the Acquisition and Inversion of NMR T_2 Data in Shales

M. Nadia Testamanti[a,*], Reza Rezaee[a]

[a] *Curtin University*
Perth, Western Australia

Abstract

Low-field Nuclear Magnetic Resonance (NMR) is a non-invasive method widely used in the petroleum industry for the evaluation of reservoirs. Pore structure and fluid properties can be evaluated from transverse relaxation (T_2) distributions, obtained by inverting the raw NMR signal measured at subsurface conditions or in the laboratory. This paper aims to cast some light into the best practices for the T_2 data acquisition and inversion in shales, with a focus on the suitability of different inversion methods. For this purpose, the sensitivity to various signal acquisition parameters was evaluated from T_2 experiments using a real shale core plug. Then, four of the most common inversion methods were tested on synthetic T_2 decays, simulating components often associated with shales, and their performance was evaluated. These inversion algorithms were finally applied to real T_2 data from laboratory NMR measurements in brine-saturated shale samples. Methods using a unique regularization parameter were found to produce solutions with a good balance between the level of misfit and bias, but could not resolve adjacent fast T_2 components. In contrast, methods applying variable regularization – based on the noise level of the data – returned T_2 distributions with better accuracy at short times, in exchange of larger bias in the overall solution. When it comes to reproducing individual T_2 components characteristic of shales, the Butler-Reeds-Dawson (BRD) algorithm was found to have the best performance. In addition, our findings suggest that threshold T_2 cut-offs may be derived analytically, upon visual inspection of the T_2 distributions obtained by two different NMR inversion methods.

Keywords: Formation Evaluation, Nuclear Magnetic Resonance, Transverse Relaxation, Porous Media, Inversion, Shale

*Corresponding author
Email address: m.testamanti@postgrad.curtin.edu.au (M. Nadia Testamanti)

1. Introduction

Nuclear Magnetic Resonance (NMR) is an established technique that has applications across a wide range of scientific disciplines, including medicine, material science and chemistry. One of the key features of this method is that measurements are non-invasive, so NMR is routinely used in the study of fluid-saturated porous media. This has proven particularly useful to the petroleum industry, where NMR tools are routinely used for the evaluation of reservoirs.

The analysis of NMR data obtained from wireline logging and laboratory measurements on cores can yield valuable information about the pore system and the different fluids present (Dunn et al., 2002; Kenyon, 1997; Freedman, 2002; Prammer et al., 1996; Coates et al., 1998). One-dimensional experiments are the most common application of the NMR technique for the study of porous media, and involve T_1 and T_2 measurements using low-field NMR spectrometers. Relaxometry experiments inspect the characteristic relaxation of the rock and fluids within its pores, which can be used to assess porosity and pore size distributions. However, a robust quantitative analysis of NMR results is essential before reliable petrophysical parameters can be derived. The narrow pores and fast relaxation rates characteristic of NMR measurements in shales generates additional challenges in NMR data acquisition and interpretation.

Different methods can be used to acquire NMR data and invert it into distributions that can yield useful petrophysical information. Previous studies have suggested different approaches for the application of the NMR technique in shales (Washburn et al., 2015), but a universal standard is still lacking. This paper will examine the influence of various methodologies on the results obtained from laboratory NMR measurements in shales, aiming to cast some light on the best practices for T_2 data acquisition and inversion. For this purpose, both experimental results from NMR measurements on shales and simulated T_2 curves will be analyzed. The T_2 data presented in Testamanti & Rezaee (2017) will then be reprocessed to illustrate how the concepts revised in the current work could be applied for the analytical determination of threshold T_2 cut-offs, which will be compared with the findings from our experimental study.

2. NMR Theory

Nuclear magnetic resonance can yield valuable information about the petrophysical characteristics of a reservoir and the different fluids present. Relaxometry experiments, in particular, are used in reservoir rocks to measure longitudinal (T_1) and transverse relaxation (T_2). The measurement of T_2 using the Carr-Purcell-Meiboom-Gill (CPMG) sequence is preferred over T_1 in porous media, mainly due to the duration of experiments and the difficulties associated with T_1 data acquisition through well-logging (Kleinberg et al., 1993).

The T_2 relaxometry technique involves an initial polarization of the nuclei in the direction of the imposed magnetic field (B_0), followed by the application of a series of radio-frequency (RF) pulses. The decaying signals emitted by the precessing nuclei, are then measured. Since the magnetization is induced on hydrogen protons, NMR logging tools are considered to yield lithology-independent results, thus avoiding the pitfalls of traditional wireline logging methods (Kenyon, 1997; Anovitz & Cole, 2015). In saturated porous media, the T_2 relaxation rates are a function of individual intrinsic (or bulk), surface and diffusion relaxation processes, governed by the equation:

$$\frac{1}{T_2} = \frac{1}{T_{2\mathrm{b}}} + \rho\frac{S}{V} + \frac{D(\gamma G T_E)^2}{12} \tag{1}$$

where $T_{2\mathrm{b}}$ is the bulk fluid transverse relaxation, ρ is the surface relaxivity, S/V is the surface-to-volume ratio of the pore, and the last term represents the diffusion induced transverse relaxation, controlled by the molecular self-diffusion coefficient (D), the magnetic field gradient (G) and the gyromagnetic ratio of the precessing nuclei (Bloembergen et al., 1948).

2.1. Data Acquisition

The CPMG Pulse Sequence

The CPMG sequence involves an initial 90° RF pulse that tips the magnetization into the transverse plane. The loss of coherence suffered by the nuclei will induce a free induction decay (FID). After a time equivalent to half an echo-spacing (T_E), a 180° pulse will refocus the spins and the spin-echo will be recorded by the NMR tool. This will then be followed by a series of 180° pulses, applied at an interval T_E, which will produce a spin-echo train, as

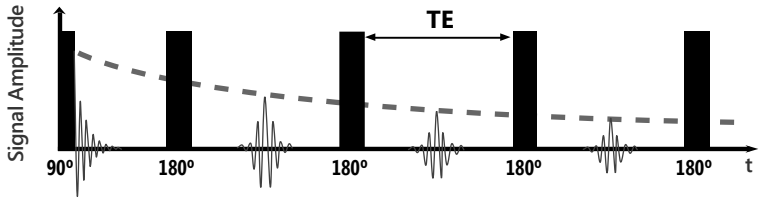

Figure 1: Schematic of the CPMG pulse sequence, used to generate an echo train during T_2 measurements (dashed line). T_E is the echo-spacing (i.e. time between consecutive 180° pulses).

illustrated in Fig. 1. It is worth noting that the dephasing caused by molecular interactions and diffusion cannot be reversed or avoided, so the CPMG pulse sequence can only be used to offset the loss of coherence resulting from B_0 inhomogeneities (Coates et al., 1999). Once a complete refocusing of all nuclei is no longer possible and the loss of coherence becomes irreversible, the spin-echo train will decay. T_2 may thus be defined as the time it takes for the nuclear spins to lose coherence with one another, and may either be shorter or equal to T_1. The T_2 decays are the primary target of NMR logging tools, from which T_2 distributions are derived by signal inversion.

2.2. Signal Processing

In NMR measurements, the decaying signals decomposed in the time domain describe a Laplace transform, which must be inverted to obtain the distribution of characteristic T_2 rates. Different approaches can be used in solving the NMR inversion problem, so the use of a suitable method is crucial for obtaining T_2 distributions that can yield meaningful petrophysical information.

In the absence of experimental errors or noise, an ideal inversion problem can be represented by a linear relationship $Y = AX$, where Y is the measured data for a given system, A is the operator describing the physics of the problem, and X includes the model parameters to estimate. Experimental noise (ξ) cannot be suppressed from real NMR measurements and, consequently, measured decaying NMR signals $m(t)$ have a structure similar to a Fredholm integral equation of the first kind (Polyanin & Manzhirov, 2008), as seen below:

$$m(t) = \int k(t, T_2)\, s(T_2)\, dT_2 + \xi \tag{2}$$

where $k(t, T_2)$ is the evaluation matrix (or *kernel*), $s(T_2)$ is the unknown spectrum. The determination of $s(T_2)$ is the key objective of the T_2 inversion process.

The integral in Eq. (2) acts as a low-pass filter that returns the smooth decaying signal $m(t)$, by attenuating the high-frequency components in $s(T_2)$. These high frequency components, along with noise, will be amplified if $s(T_2)$ is directly estimated by the inversion of the recorded data $m(t)$. Small perturbations in the measured data could lead to great variations in the spectra obtained, and such solutions are therefore said to be unstable. Furthermore, multiple distributions could produce similarly shaped T_2 decays (and vice versa) in the 1D-NMR inversion problem. Since the uniqueness and stability of solutions cannot be guaranteed, the NMR inversion problem is considered as *ill-posed*. In such cases, where a straightforward inversion to solve the problem stated in Eq. (2) is not possible, estimating the T_2 spectra requires a different approach that includes the use of regularization techniques (Polyanin & Manzhirov, 2008). The inversion of T_2 signal decay must be transformed into a numerical optimization problem that can admit a unique solution, ensured by the introduction of constraints. The T_2 distribution will then be determined as the solution that best fits the measured data (under certain constraints).

Discretisation

The raw data recorded during NMR measurements is a complex signal, sampled at intervals T_E; however, only the real part of the NMR signal is generally used for further analysis in spectroscopy (Rutledge, 1996). The continuous integral in Eq. (2) can be transformed into a linear algebraic system by discretization, taking the form:

$$M = KS + E \tag{3}$$

where the vector $M \in \mathbb{R}^m$ contains the data acquired at times t_i, $K \in \mathbb{R}^{m \times n}$ is the kernel, $S \in \mathbb{R}^n$ is the distribution evaluated for the relaxation times T_{2j}, and $E \in \mathbb{R}^m$ is the error (or noise). In saturated rocks, the relaxation components are assumed to decay exponentially, so Eq. (3) can be rewritten as:

$$m_i = \sum_{j=1}^{N} s_j \, e^{-(t_i/T_{2j})} \quad i = 1, 2, ..., M \tag{4}$$

where the relaxation times T_{2j} are typically logarithmically spaced (Borgia et al., 1990; Whittall, 1996).

Singular Value Decomposition

The stability and computing cost of the NMR inversion problem can be improved by projecting the data onto a subspace, defined from a truncated singular value decomposition (SVD) of the kernel matrix (Mitchell et al., 2012; Hürlimann & Venkataramanan, 2002; Song et al., 2002; Venkataramanan et al., 2002). The matrix K can then be factorized by means of SVD:

$$K = U\,\Sigma\,V^T \tag{5}$$

where $U \in \mathbb{R}^{m\times m}$ and $V \in \mathbb{R}^{n\times n}$ are orthogonal singular matrices, and $\Sigma \in \mathbb{R}^{m\times n}$ is a diagonal matrix of the singular values in descending order (Hansen, 1987).

The next step involves the compression of data by truncating the singular values in Σ. The inclusion of a large number of values enhances the effect of noise in the spectrum, but limiting their number when the signal-to-noise ratio (SNR) is low may lead to solutions with artificially broad peaks (Song et al., 2005). Thus, only the first components of Σ that hold significant information should be retained, while those that contain mostly noise are to be discarded. The number of significant singular values $\tilde{n}_r$ depends on the condition number, calculated as the ratio of the largest to smallest singular values in the rank reduced Σ_r. The truncation level is commonly determined based on the signal-to-noise ratio of the data (Mitchell et al., 2012; Song et al., 2005), and should satisfy the necessary conditions to ensure well-conditioned matrices (Hansen, 1987). The truncated matrices will be U_r $(m \times r)$, Σ_r $(diagonal,\ r \times r)$, V_r $(n \times r)$. The compressed data vector will then be calculated as $M_r = U_r^T M$, and the reduced kernel is $K_r = \Sigma_r V_r^T$.

The truncated SVD approach can be used for regularization, but requires previous knowledge about the solution to identify the optimal truncation value and cannot guarantee positive solution elements, and should thus be used in combination with other methods (Venkataramanan et al., 2002).

The NMR Optimization Problem

The NMR data inversion process is equivalent to finding the best possible solution to an optimization problem. Additional constraints are imposed on the algebraic system, to ensure that the T_2 spectra obtained is physically representative of the real NMR phenomena in porous media. Since multiple possible solutions could fit the observed data relatively well, several numerical methods have been proposed to find the best possible result. The techniques most commonly used for NMR inversion are described below.

The problem described by Eq. (3) can be solved with the non-negative least squares (NNLS-LH) method proposed by Lawson & Hanson (1974). In the NNLS-LH method, solutions are obtained by minimizing the misfit between measured (M) and predicted data ($K\,S$), subject to non-negativity constraints. Based on the dimensionality reduction previously explained, the NMR problem can be written as:

$$\underset{S_r \geqslant 0}{\arg\min} \parallel M_r - K_r\, S_r \parallel_2^2 \tag{6}$$

where $\parallel \cdot \parallel_2^2$ is the squared Euclidean L_2 norm. The NNLS-LH method is very stable, but convergence can be slow and solutions may consist of only a few isolated components, as opposed to the smooth distributions associated with NMR relaxation in porous media (Whittall, 1996). Furthermore, solutions are quite sensitive to noise so adjacent peaks may be merged during the inversion process (Whittall, 1994).

The solutions to the general NMR inversion problem are generally found based on the methodology introduced independently by Twomey (1963) and Tikhonov (1963), which addresses both the non-negativity and smoothness requirements. In this method, a penalty smoothing term $\parallel L\,S_r - S_{r\,0} \parallel_2^2$ is included to avoid solutions featuring numerous sharp peaks that are not physically representative (despite being a good numerical fit). The problem described by Eq. (6) is then extended to:

$$\underset{S_r \geqslant 0}{\arg\min} \parallel M_r - K_r\, S_r \parallel_2^2 + \lambda \parallel L\, S_r - S_{r\,0} \parallel_2^2 \tag{7}$$

where L is the regularization operator (matrix of additional constraints), and λ is a variable known as the regularization parameter. The L operator can regularize the solution via

an L_0, L_1 or L_2 norm penalty function, often referred to as norm (or energy), slope or curvature smoothing (Dunn et al., 1994). The tuning parameter (λ) in Eq. (7) regulates the smoothness of the solution relative to the misfit term. Larger values of λ will dampen the smallest significant singular values (associated with noise) and thus lead to smoother solutions. The incorrect selection of the regularization parameter λ can result in either under or over-smoothed spectra, so several methods have been developed to find the optimal λ_{opt} that provides the best trade-off between misfit and smoothness of solutions to return realistic T_2 distributions.

The Tikhonov regularization described by Eq. (7) may be implemented using a direct (forward) or an indirect approach. The direct methodology involves an initial analysis to determine the optimal regularization parameter which is later used to calculate the best possible solution, often using the NNLS-LH method (Lawson & Hanson, 1974). In contrast, the indirect approach finds the solution to the NMR problem with the help of auxiliary functions, such as the method proposed by Butler et al. (1981). Four methods for determining λ_{opt} are presented below: the *L-curve*, *GCV*, *BRD* and *UPEN*.

Choice of Regularization Parameter

The *L-curve* method, proposed initially by Lawson & Hanson (1974) and further developed by Hansen (1992) and Hansen & O'Leary (1993), was one of the first algorithms introduced to solve the NMR inversion problem. The plot of the solution norm versus its corresponding residual norm, as a function of a given range of λ values results in an L-shaped curve as illustrated in Fig. 2, giving its name to this method. The point at which the slope of the curve abruptly changes is then selected as the optimal smoothing coefficient λ_{opt}. The selection of the best regularization parameter may thus be somewhat arbitrary with the L-curve method, depending on the data analyzed.

The *generalized cross-validation* (GCV) method, proposed by Golub et al. (1979), finds the optimal regularization parameter λ_{opt} that minimizes the function:

$$GCV(\lambda_{opt}) = \frac{\| M_r - K_r S_{r,\lambda} \|_2^2}{[\text{trace}\,(\mathbb{I} - S_{r,\lambda})]^2} \tag{8}$$

where $\mathbb{I}$ is the identity matrix, and $S_{r,\lambda}$ is the solution calculated for a certain smoothing

coefficient λ.

In the *Butler-Reed-Dawson* (BRD) method, an auxiliary convex function is minimized to find the λ_{opt} (instead of performing direct iterations over c_r) based on the discrepancy principle (Butler et al., 1981; Morozov, 1984). The regularization parameter may be empirically determined as a function of a specified level of misfit in the data, such as RMSE. It is also common for solutions to be obtained based on the SNR of the data, generally defined as SNR $= M(0)/\sigma$, where σ is the noise standard deviation (Song et al., 2005). Using the Newton method, the estimated λ values are updated stepwise as a function of $\sqrt{n_r}/ \parallel c_r \parallel$ (Mitchell et al., 2012), and the misfit error is calculated as:

$$\chi(c_r, \lambda) = \frac{\lambda \parallel c_r \parallel}{\sigma} \tag{9}$$

The S-curve is commonly used to find the optimal regularization parameter, which evaluates the sigmoidal shape displayed in the log-log graph of the misfit error, as a function of λ (Fordham et al., 1995). The optimal solution is found at the "heel" of the S-curve, where λ satisfies:

$$\frac{d(\log \chi(c_r, \lambda))}{d(\log \lambda)} = \text{TOL} \tag{10}$$

for a predetermined tolerance value (TOL) selected by the user.

The *UPEN* method proposed by Borgia et al. (1998) uses a quadrature regularization function, where λ varies with the relaxation time to obtain a uniform application of the smoothing penalty term. The method was later refined, introducing a combination of regularization functions to effectively obtain a variable smoothing (Borgia et al., 2000). In the second version of the UPEN method, the averaged signal within a defined window and the corresponding weight factors are used to provide feedback for a uniform penalty smoothing.

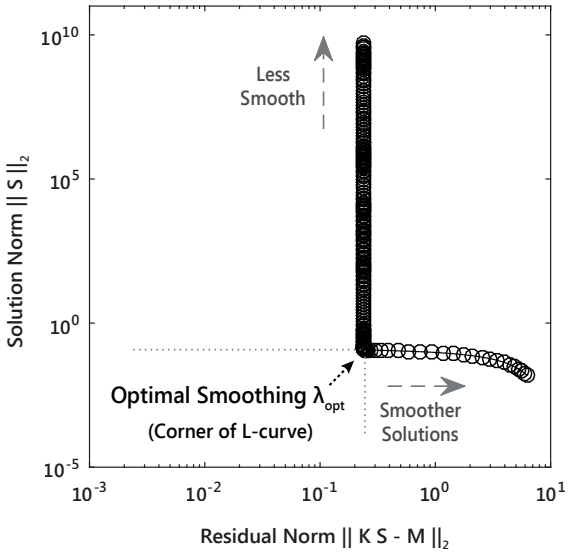

Figure 2: Graphical analysis of the solution norm $\| s \|_2$, calculated for discrete regularization parameter values (λ) and plotted against the corresponding residual norm $\| KS-M \|_2$, known as the L-curve method. The horizontal part of the curve indicates the residual norms that are most sensitive to errors arising from the incorrect selection of λ. The vertical part illustrates the solution norms that are most sensitive to errors associated with amplification of random noise. The optimal λ_{opt} is found at the corner of the discrete L-curve, either visually or based on a numerical method such as the adaptive pruning algorithm (Hansen, 2015).

3. Methodology

Experimental results from NMR measurements conducted in shales and simulated T_2 decay curves were utilized to study the impact of different variables involved in the NMR signal acquisition and inversion process.

In Subsection 4.1, the impact of various acquisition parameters on the T_2 signal measured in shales is analyzed. All NMR experiments were performed on a 2 MHz Magritek Rock Core Analyzer set to 30°C, equipped with either a P29 or P54 probe and using different settings. The real T_2 decays presented in this subsection were obtained on the same 1" diameter core plug, in the *as-received* state, which was tightly wrapped in a plastic film to prevent moisture evaporation or absorption. The sample belongs to the Carynginia Formation, a dry gas-prone shale section found in most of the northern Perth Basin (Mory & Iasky, 1996).

The inversion methods included in the previous section of this paper are tested on synthetic T_2 data, as shown in Subsection 4.2. The T_2 decays were generated to replicate the equivalent relaxation response that would be obtained from measurements conducted in real shale samples. The *Lexus* module in the Prospa software (Magritek) was used for the BRD inversions, whereas the NNLS-LH/L-curve, NNLS-LH/GCV and UPEN algorithms were implemented in Matlab (Mathworks), using purposely written code. In the latter case, final computations were done using the NNLS function included in the MERA Toolbox for Matlab (Does, 2014).

In Subsection 4.4, the four inversion methods are then tested on real NMR data. The raw T_2 decays were originally obtained from brine-saturated core plugs, in the experimental study presented in Testamanti & Rezaee (2017). The T_2 decays were acquired using 10,000 echoes and a 100 µs echo time, with the magnet temperature set to 30 °C. The number of scans was automatically adjusted to collect data with a minimum SNR of 200 and the background signal – corresponding to the probe and plastic wrap – was subtracted from the total measured T_2 decays. The raw data was phased using the Prospa software (Magritek) to maximize the contribution from the real component in the signal, later used for inversion. More information on the geological background of these six samples and preparation procedures can be found in the original paper (Testamanti & Rezaee, 2017).

4. Results and Discussion

4.1. T_2 Data Acquisition

As reviewed in the previous section, the CPMG sequence involves an initial polarization of the nuclear spins, followed by the application of a series of magnetic pulses N_E, spaced by a T_E time. Consecutive CPMG pulse trains are separated by a wait time or inter-experimental delay (T_W), during which the polarization of the system builds up. The parameters N_E, T_E, T_W, as well as the pulse specifications, are all necessary inputs of T_2 CPMG experiments and must be suitably chosen by the user. The output will be a vector with the raw T_2 data, recorded at fixed intervals T_E. The impact of various acquisition parameters on results is discussed below.

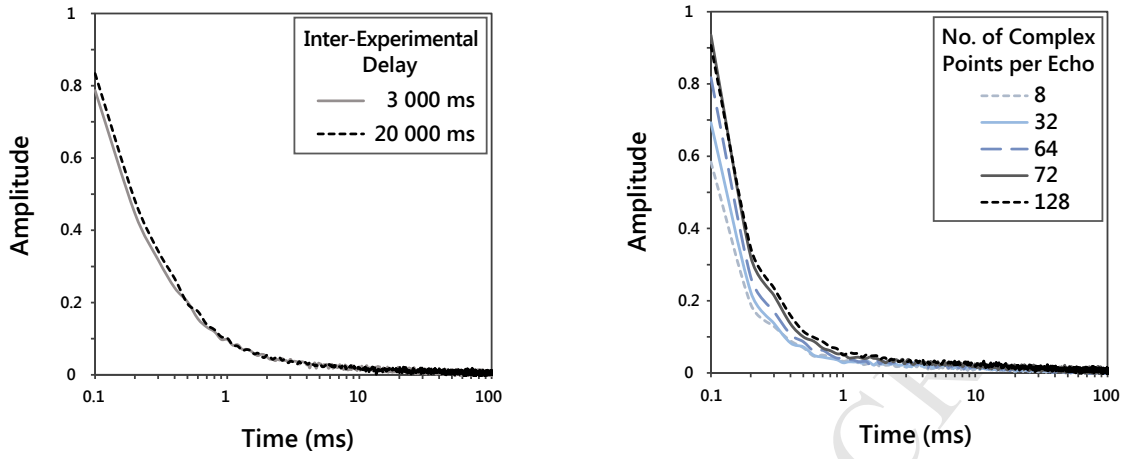

(a) (b)

Figure 3: T_2 decay curves showing (a) the effect of the inter-experimental delay parameter on M(0); (b) the influence of the number of complex points sampled per echo on signal quality.

Inter-Experimental Delay

The magnitude of M_0 is estimated from the signal amplitude measured after the first RF pulse in the sequence. Thus, T_W should be set to at least three times the expected T_1 value, to allow a 95% polarization of the spins and avoid underestimating M_0. Shales have very fast relaxation rates, so generally short T_W times can be safely used for T_2 measurements. This is illustrated in Fig. **??**, where the impact of the inter-experimental delay parameter on the measured M_0 of a shale core sample is examined. The T_2 decays were acquired with the P54 probe for 3,000 echoes, with a $T_E = 100$ µs and the same target SNR = 220 but using short and long T_W values, set to 3,000 and 20,000 ms respectively. Similarly shaped T_2 decay curves emerge from the graph, while the difference between the calculated M_0 was about 7%. The use of longer inter-experimental delays was thus found to only marginally improve the estimation of M_0 values. The impact of the T_W parameter on the overall duration of measurements, however, becomes more significant in shales and should be evaluated against time constrains if applicable.

Signal-to-Noise Ratio

Despite being relatively weak, NMR signal can be detected in rocks owing to the abundance of hydrogen protons in the reservoir fluids. Improving the quality of NMR data

measurements can be seen as equivalent to reducing the experimental noise, which improves the effective SNR of the data. After signal is detected, the in-phase and quadrature signals for each spin-echo are sampled, according to the number of complex points and dwell time set by the user, and digitized in the spectrometer before returning to the computer (Kleinberg, 1999). To enhance the quality of the results, a signal averaging – or stacking – process is performed on the raw data, followed by a phase correction. The final outputs are two data vectors, one containing the real components of the spin-echo train from which T_2 distributions will be obtained, and another containing the imaginary portion of the complex signal that represents the noise with zero mean (Coates et al., 1999).

The acquisition of a large number of echoes N_E allows the decay of real components in the signal to noise level, ensuring the detection of all the T_2 relaxation rates present in the core sample. In practice, the experimental settings should satisfy the condition $N_E \geq T_{2,\max}/3T_E$ to detect the full range of T_2 components (Coates et al., 1999). As observed in Fig. **??**, shales have fast relaxation rates so most of the signal should be captured within the first few hundred milliseconds.

The SNR of the acquired data may be enhanced by performing a signal averaging or stacking. This technique relies on the random feature of noise, as opposed to the reproducibility of the NMR signal, and therefore cannot filter out coherent noise. By averaging the signal from a number of successive scans N, the amplitude will grow at a rate of N whereas the growth rate of noise will be $\sqrt{N}$. The SNR improvement will then be proportional to $\sqrt{N}$ averaged, where the number of scans should be a multiple of 4 for a full phase cycling. Another method often used to enhance the SNR consists in increasing the number of complex points sampled per echo. The product of this sampling number (ideally a power of 2) and the dwell time will determine the total acquisition time (T_{acq}) for each spin-echo; the spectral width is given by the reciprocal of the dwell time. The minimum T_E available for the instrument will be limited by the acquisition time, and should be greater than T_{acq} plus an added delay to avoid artifacts in the signal due to the acoustic ringing of the probe. Nonetheless, the law of diminishing returns applies to both of the SNR enhancement techniques previously described and should be carefully considered when experimental parameters are selected. The acquisition of a large number of points per echo may overheat the RF amplifier and thus damage the instrument, while an increase in the

number of scans can extend the duration of experiments considerably. Fig. 3b shows the T_2 curves obtained from CPMG sequences on a real shale core sample, where the raw signal was sampled using a variable number of complex points. Measurements were conducted using Magritek's P29 probe, with 2,000 echoes and a $T_E = 100$ µs. Increasing the number of complex points sampled per echo from 8 to 32 leads to a 15% rise in the initial signal amplitude, similar to increasing the sampled points from 32 to 64, and then from 64 to 72. No substantial variations are observed between the curves acquired with 72 and 128 points per echo. The proportional rise in the noise standard deviation, however, prompts to question whether the increase in the first few data points could be in fact an artificial enhancement, caused by acoustic ringing effects (Gerothanassis, 1987). The use of a long acquisition delay is often recommended to prevent the collection of spin-echoes distorted by the probe free ringing, but that could also lead to the loss of valuable information in tight porous media. Since most of the signal decay generally occurs in the first few data points, the use of post-acquisition filters and alternative data fitting techniques that can compensate for offset and acoustic ringing effects may be more suitable for processing NMR data in shales (Freedman, 2002; Venkataramanan et al., 2013; Salimifard et al., 2017).

Alternatively, the use of relatively larger core samples, where hydrogen nuclei are more abundant, can yield an improvement of the signal quality. Since this is not always possible, the use of instruments with smaller RF coils could be another option for achieving higher SNR levels during measurements.

Echo-Spacing (T_E)

The use of shorter T_E enables the earlier detection of NMR signal, desirable in the case of rocks with fast relaxing components. The number of complex points sampled per spin-echo, the pulse length and the acquisition bandwidth – along with the instrument's characteristics – will limit the minimum echo time that can be used for measurements. SNR will generally increase with decreasing T_E, as more data points will be generated (and recorded) at shorter intervals. The reduction in T_E also has the unintended consequence of accentuating acoustic ringing effects. The first echoes are generally more affected by the acoustic ringing of the probe which would consequently become part of the recorded signal, causing a very high initial amplitude followed by a coherent transient (Coates et al.,

1999). This effect can be observed in Fig. 4a, where the background signal acquired with a T_E of 40 µs shows a higher initial amplitude, compared to the value obtained at a 100 µs echo-spacing.

The ringing noise can be filtered out to some extent by manipulating the digital filter bandwidth, at the expense of loss in sensitivity owing to the limitations on the minimum T_E possible (Salimifard et al., 2017), or attenuated by the use of smaller probes. The effect of random noise can be mitigated by simply subtracting the NMR signal corresponding to the instrument, from measurements on core samples. While background noise generally has little impact on results from high porosity rocks, it can contribute substantially to the NMR signal measured in shales (Saidian, 2015; Salimifard et al., 2017). It is therefore good practice to obtain the background signal emitted by sample containers or plastic wraps and by the instrument itself, which should be then subtracted from the T_2 decays – prior to data inversion. The effect of subtracting the background signal from T_2 measured on a real shale core sample is illustrated in Fig. 4b, where experiments were conducted at 40 µs and 100 µs echo-spacings using a P29 probe. A greater portion of the fast T_2 components could be detected using a shorter T_E, although this difference becomes less significant beyond 0.5 ms. These fast T_2 relaxation rates are typically associated with organic and inorganic micropores, so short echo-spacings should be used whenever possible to investigate the full range of pore size ranges found in the shale matrix.

A final point to consider is the issue of thermodynamic stability, crucial for T_2 measurements based on the CPMG pulse sequence. In core samples where narrow pores are abundant, the duration of experiments can increase considerably and span several hours. Failure to achieve isothermal conditions could lead to the underestimation of M_0, so core samples should always be allowed to stabilize to the magnet temperature prior to measurements. Alternatively, samples could be pre-heated before loading them into the spectrometer, provided that they are tightly sealed to avoid unintended fluid loss due to vaporisation.

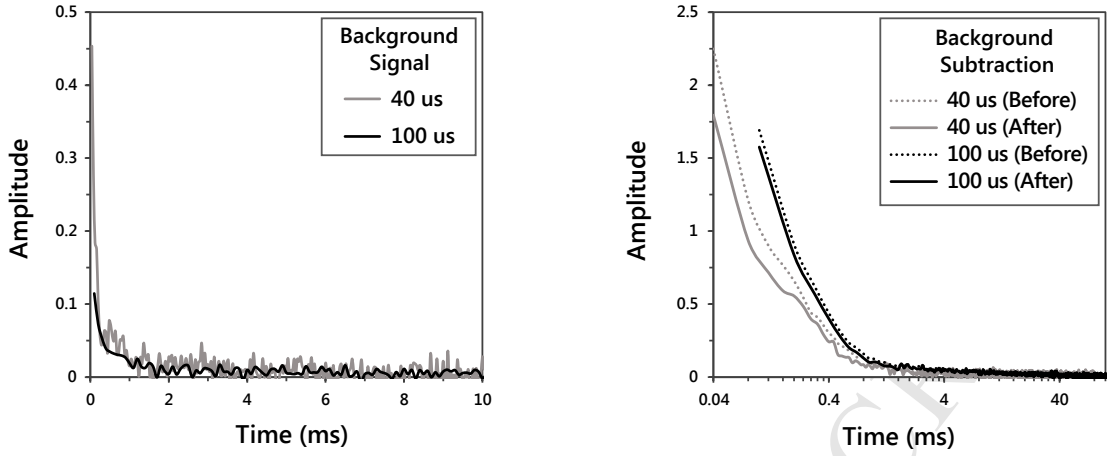

(a) (b)

Figure 4: T_2 decay curves showing **(a)** the background signal measured; **(b)** the effect of removing the background noise from the main signal, acquired at different echo-spacing. Measurements conducted using Magritek's P29 probe.

4.2. T_2 Data Inversion

The ultimate goal of the T_2 inversion process is finding the spectrum that best represents the real relaxation mechanisms in the saturated porous media. Most NMR inversion methods can correctly find solutions for systems where the dominant T_2 components are sufficiently separated, so the choice of the inversion algorithm is not a significant source of concern. This, however, is not usually the case in complex porous systems with abundant small pore sizes such as shales. The shale matrix typically has a substantial clay and organic content, with protons susceptible to magnetization that yield fast T_2 relaxation rates, often generating most of the total NMR signal acquired. Inversion algorithms must be therefore carefully selected, as the reconstructed signal should include sharper peaks at short T_2 times, which are associated with the relaxation of fluids in the smaller pores, clay bound water and solid organic matter present in shales. Caution must be nonetheless applied, to avoid artifacts in the spectrum at longer T_2 times that may not be representative of real nuclei relaxation within the larger pores.

The inversion algorithms described in the previous section were tested on a set of simulated T_2 decays emulating the relaxation rates commonly associated with sandstones and shales, designated as case A and B in this study. The T_2 curves were obtained from syn-

thetic distributions with the following distinctive features: (A) three peaks, centred on 2, 14 and 44 ms, displaying maximum normalized amplitudes of 20%, 50%, and 30% respectively; (B) four peaks, centred on 0.1, 2, 14 and 44 ms, displaying maximum normalized amplitudes of 20%, 40%, 30%, and 10% respectively. The T_2 components used as input for the simulations are indicated with black lines in Fig. 5. The T_2 decays were generated for 3,000 and 10,000 echoes, based on a 100 µs echo time. Gaussian noise was also added to the raw T_2 decay curves, to obtain SNR levels comparable to those of the experimental NMR data presented in the previous subsection.

Data Compression

Before inversion, the size of acquired data is reduced for computational efficiency purposes and to filter out noisy values. The initial compression of NMR data can be computed with the TSVD method, which requires the selection of an optimal truncation value (Venkataramanan et al., 2002). Choosing this threshold incorrectly can lead to substantial attenuation of the shortest T_2 (Prammer, 1994; Song et al., 2005), and consequent loss of valuable information in systems where fast components are expected. If a large number of singular values are kept before inversion, the identification of individual adjacent peaks in the T_2 spectrum could be compromised and lead to distributions featuring one broad peak at short T_2 times. In shales, the earliest raw data points will likely contain the most valuable information and must be preserved, whereas the noisy part of the T_2 curve should be pruned before inversion. The truncation criteria also becomes more critical as the size of acquired data increases, relative to the time vector on which the inversion is evaluated. The data compression methodology can therefore have a more significant impact on results obtained in shales, compared to other types of reservoirs. In this study, the optimal number of significant singular values to preserve for the inversion were examined based on the L-curve method described in Hansen et al. (2007). The algorithm was implemented in Matlab (MathWorks), using the Regularization Toolbox (Hansen, 2015). For the simulated T_2 decays, a prune to between 25–50 significant values was generally found to produce stable solutions.

Inversion Method

The incorrect selection of NMR inversion algorithms could potentially lead to gross interpretation errors, especially when the T_2 spectra are correlated to porosity and pore size distribution obtained from other core analysis methods. To assess the influence of inversion algorithms on shale results, the simulated T_2 curves were inverted for a logarithmically spaced vector with 200 points, within the range 0.01–600 ms for data simulated with 3,000 echoes, and between 0.01–2,000 ms for the cases with 10,000 echoes. Solutions were regularized with the energy of the T_2 spectrum, also know as norm-smoothing, except for inversions based on the UPEN method where curvature-smoothing was used instead. For the forward inversions using the NNLS-LH method, the optimal smoothing coefficients were chosen based on the L-curve (continuous blue line) and GCV criteria (light blue line), whereas distributions obtained by indirect approaches were computed with the BRD (dashed grey line) and UPEN algorithms (dotted grey line). The resulting T_2 distributions by the different methods are presented in Fig. 5, while the signal intensities are included in Table 1. The goodness of fit of the different inversion methods were evaluated by the sum of absolute error (SAE), root-mean squared error (RMSE), peak signal-to-noise ratio (PSNR) and structural similarity index (SSIM) (Wang et al., 2004; Miao et al., 2008); the residual statistics are summarized in Table 2.

For the case A, no significant differences are observed between the total signal simulated, recovered and calculated by the four NMR inversions, irrespective of the number of echoes (Table 1). In contrast, about 15% of the NMR signal in the simulated spectrum B is lost by the use of a 100 µs echo time (which allows only a partial detection of the peak centred on 0.1 ms), while the acquisition of a larger number of echoes has a minor positive effect on the total amount of signal recovered. The comparison of case B results reveals that the BRD and UPEN algorithms can closely reproduce the original T_2 signal recovered (13.01 and 13.19 for 3,000 and 10,000 echoes, respectively), with an error $< 0.5\%$. The differences between the original and inverted signal intensities are greater for the NNLS-LH method, based on both the L-curve (1–2%) and GCV criteria (2.5–4.5%).

Fig. 5 shows that – in all cases – direct inversion approaches (NNLS-LH combined with L-curve and GCV methods) yields smoother T_2 spectra than the BRD and UPEN algorithms. In conventional reservoirs, smooth solutions featuring broad spectral peaks

are generally considered to be physically representative of the saturated porous media, and therefore selected as the best fits. On the other hand, solutions including sharp peaks are typically discarded, while strong signals at short relaxation times are often attributed to noise magnification effects. Based on common practice, T_2 curves determined by the combination of the NNLS-LH method with either the L-curve or GCV are generally less biased and would thus be preferred for evaluating petrophysical properties. However, the use of a single regularization parameter in systems where adjacent peaks have different widths and amplitudes may also lead to either excessive broadening of narrow features, or sharpening of broad peaks (Borgia et al., 1998). This effect becomes apparent in all the T_2 distributions obtained by NNLS-LH inversion with either the L-curve or GCV techniques, as the λ_{opt} could not correctly resolve the adjacent components centred on 12 and 44 ms. Instead, the individual features seem to emerge as a combined unique broad peak, visible in all the T_2 spectra generated by direct inversion approaches. Since the NMR signal measured in shales will exhibit a sharp decay at short T_2 times where high experimental SNR levels are often unattainable, the lack of sensitivity to noise of the NNLS-LH inversion method is certainly a source of concern. Separating the contributions from individual fast relaxing T_2 components would likely be difficult with the use of inversion methods that apply a fixed amount of smoothing (e.g. NNLS-LH), however, the solutions would also be less biased and therefore more representative of global properties such as NMR porosity. On the other hand, noise-sensitive algorithms (e.g. BRD) may extrapolate the NMR signal well below the detection limit of the spectrometer and introduce significant bias in the determination of T_2 spectra, but could also help to distinguish individual adjacent peaks. This particular attribute could facilitate the identification of threshold T_2 cut-offs, as will be discussed later in this paper. These threshold parameters may ultimately be applied to experimental T_2 data, from which the porosity fractions associated with bound (BVI) and free fluids (FFI) can be estimated (Coates et al., 1999; Prammer et al., 1996; Chen et al., 1998).

Turning now to the overall accuracy of each method, it is evident from Fig. 5 that the contribution of individual peaks to the final T_2 spectra cannot be accurately distinguished by the use od forward inversion methods. The particular features in the simulated NMR data disappear after the NNLS-LH/GCV inversion (cases A & B), while the NNLS-LH/L-curve algorithm returns seemingly better fits with more precise peak locations (case B).

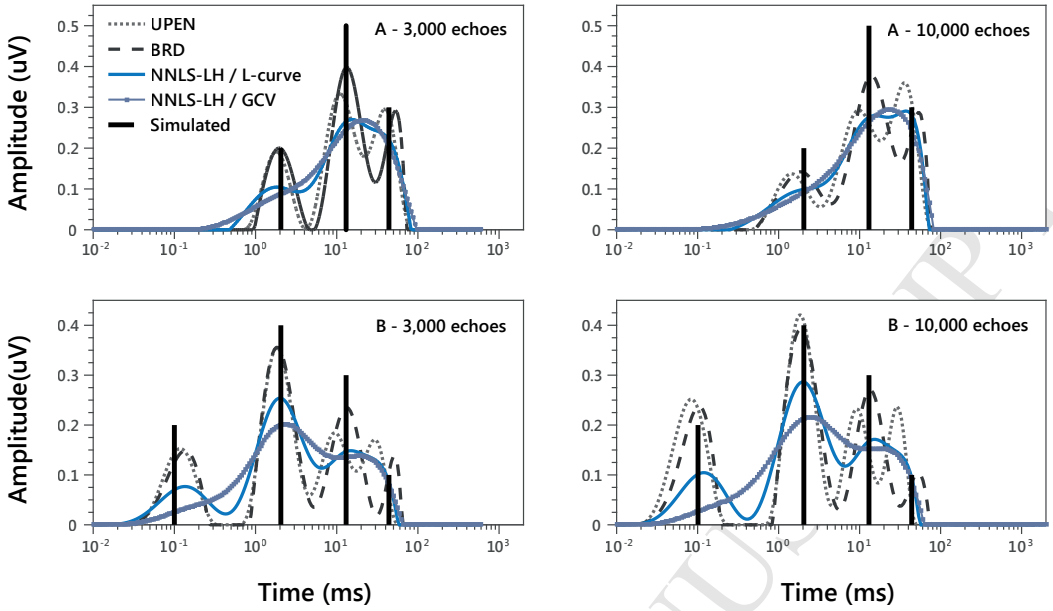

Figure 5: T_2 spectra from simulated decay curves for 3,000 (left panel) and 10,000 echoes (right panel), inverted with the NNLS-LH/Lcurve, NNLS-LH/GCV, BRD and UPEN methods. The black vertical lines indicate the T_2 components from which the decays were generated.

Interestingly, the NNLS-LH/L-curve produces larger residuals than the NNLS-LH/GCV inversion, and has poorer PSNR, RMSE and SSIM scores (Table 2). The global performance of the NNLS-LH/L-curve method seems to improve when the number of echoes acquired increases (case B), matching the inversion quality metrics of the NNLS-LH/GCV algorithm. On the other hand, indirect NMR inversion approaches return T_2 spectra displaying well-defined peaks. The BRD algorithm produces the best fits, in terms of both locating and estimating the amplitudes of the main peaks. The UPEN method is able to preserve the details of the original simulated data but fails to determine peak locations and amplitude correctly, while the weak associated PSNR, RMSE and SSIM scores render it the least reliable method out of the four herein analyzed. Overall, the best fits are obtained with the BRD method, as confirmed by the superior inversion quality metrics. Surprisingly, the acquisition of a larger number of echoes appears to negatively impact the T_2 inversions on the simulated dataset A, while positive effects are observed on the dataset B results.

Table 1: Comparison of NMR signal intensities for the simulated T_2 data sets, obtained by the NNLS-LH with L-curve, NNLS-LH with GCV, BRD and UPEN inversion methods.

Sample	No. Echoes	Original	Recovered	NNLS-LH (L-curve)	NNLS-LH (GCV)	BRD	UPEN
A	3,000	13.69	13.44	13.46	13.45	13.45	13.42
A	10,000	13.69	13.47	13.48	13.42	13.51	13.45
B	3,000	15.32	13.01	12.85	12.67	13.01	12.95
B	10,000	15.32	13.19	12.96	12.64	13.18	13.14

Table 2: Goodness of fit for the simulated NMR data sets, inverted with the NNLS-LH/L-curve, NNLS-LH/GCV, BRD and UPEN methods. Quality of the inversion is assessed by the sum of absolute error (SAE), root-mean squared error (RMSE), peak signal-to-noise ratio (PSNR) and structural similarity index (SSIM). Errors are computed as the residuals between the initial data (M) and the predicted decay curves from each method ($M^p = KS_{\text{reg}}$). Low RMSE, and high PSNR and SSIM values are indicative of good quality inversions.

Sample	No. Echoes	Original	NNLS-LH (L-curve)	NNLS-LH (GCV)	BRD	UPEN
				SAE ($\times 10^2$)		
A	3,000	8.22	1.57	1.50	1.46	1.71
A	10,000	18.70	5.48	5.39	5.16	5.67
B	3,000	4.15	1.67	1.63	1.39	1.82
B	10,000	10.16	5.40	5.37	5.03	5.56
				PSNR		
A	3,000	241	234	238	241	227
A	10,000	236	231	232	236	228
B	3,000	245	229	231	244	222
B	10,000	239	233	233	239	231
				RMSE ($\times 10^{-2}$)		
A	3,000	41.12	6.76	6.46	6.24	7.33
A	10,000	36.95	7.01	6.91	6.59	7.25
B	3,000	21.83	7.13	7.02	6.02	7.72
B	10,000	19.27	6.83	6.83	6.39	7.02
				SSIM		
A	3,000	0.96	0.95	0.96	0.96	0.95
A	10,000	0.89	0.88	0.88	0.89	0.88
B	3,000	0.94	0.91	0.92	0.94	0.90
B	10,000	0.88	0.87	0.87	0.88	0.86

4.3. Relaxation Mechanisms in Shales

Hydrogen-rich particles confined to a bounded domain are often abundant in organic shales. Micro-porosity associated with kerogen, clays and particles adsorbed to the surface of the pore has a solid-like appearance from an NMR tool perspective (Washburn, 2014). These quasi-rigid molecules are typically absent in conventional reservoir rocks, where surface relaxation mechanisms are considered to dominate the measured T_2 signal decay provided that the applied magnetic field is homogeneous (Coates et al., 1999; Kleinberg, 1999; Kenyon, 1997). In very tight porous media, however, Brownian processes may arise from the abundance of molecules confined to a virtually restricted domain. The diffusing spins in a quasi-solid state would follow an approximately motional-narrowing regime that can be described by a Gaussian distribution, influencing the shortest T_2 components in shales (Grebenkov, 2007; Washburn et al., 2015).

One of the inherent issues with NMR experiments is the limitation of signal acquisition in time, which could give way to distortions in the inverted spectrum that may appear as "feet" on either side of true peaks (Eveleigh, 1996). These distinctive signatures could be the result of signal "leaks", or in fact correspond to a separate peak that cannot be entirely detected owing to spectrometer limitations. The challenge is then to determine whether these features in the T_2 spectra are artifacts or if they have an actual physical meaning. For instance, relaxation rates below the first spin echo acquired are customarily excluded from the NMR data inversion, yet their decaying signal may still be partially detected on the earliest data points. If the mean of the fastest relaxing component is relatively close to the first T_2 data point acquired and measurement conditions ensure a high enough SNR, then some extrapolation can be safely done below the first real T_2 component (Moody & Xia, 2004). Furthermore, the actual detection of components below the threshold of the NMR instrument might be possible if stochastic resonance is generated. This naturally occurring phenomenon could be exploited by the dithering technique to amplify experimental noise and enhance the signal from very fast T_2 components that would generally be too weak to be detected (Pearce et al., 2008). Nonetheless, distinguishing between fast relaxing T_2 components produced by real relaxation mechanisms and those associated to ringing noise, would likely be an impossible task.

The degree of heterogeneity associated with shales, often displaying a wide separa-

tion between the smallest and largest length scales, favors the broadening of features in the T_2 spectra (Watson & Chang, 1997). Additionally, the intricate shale pore network may induce large internal magnetic field gradients and thus the Brownian motion of spins, leading to deviations from the fast diffusion regime (Hürlimann, 1998; Song, 2000, 2003; Washburn, 2014). These diffusion effects can be quantified based on laboratory 2D–NMR experiments, from which T_2 data corrections may be derived and the contribution from diffusion-induced signals estimated (Sun & Dunn, 2004). Unfortunately, obtaining sound results from borehole measurements remains impractical in shale reservoirs with the technology currently available, owing to the high levels of noise and consequently low SNR, and T_2 experiments therefore remain as the most viable NMR data source to yield petrophysical information. One final point to consider is the impact of non-negligible internal gradients on the accuracy of NMR porosity determination, which may lead to its overestimation (McPhee et al., 2015). To minimize gradient-induced T_2 relaxation effects in shales, the use of the use of larger core samples, low field spectrometers and short echo-spacings in the CPMG sequence, is recommended.

4.4. Comparison of NMR Inversion Methods for the Analytical Determination of Threshold T_2 cut-offs

Our previous paper (Testamanti & Rezaee, 2017) presented a methodology for the experimental determination of threshold T_2 cut-offs in shales, based on the analysis of cumulative NMR porosity curves which were acquired on brine-saturated, centrifuged and oven-dried core plugs (Fig. 6). In that study, two experimental threshold $T_{2\ \text{cut-off}}$ were identified after the samples were centrifuged and oven-dried: an upper T_{2U} (in the range 1–2 ms) and a lower T_{2L} (between 0.2–0.3 ms), respectively. In this current section, we will show that these threshold T_2 cut-offs could also be derived analytically, from the comparison of T_2 distributions obtained by two different NMR inversion methods. The four inversion methods applied on the synthetic T_2 data were thus used to reprocess experimental T_2 decays, which were obtained from brine-saturated shale core plugs as part of our previous study (Testamanti & Rezaee, 2017).

The T_2 decays were initially processed based on the NNLS-LH method, using the Lawson and Hanson module in the Prospa software (Magritek), by which the T_2 distributions

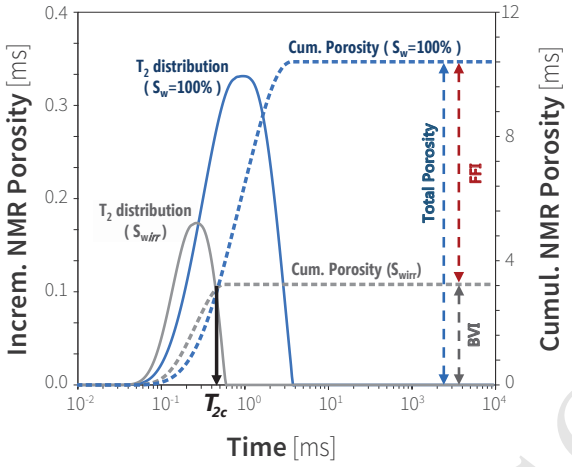

Figure 6: Methodology used in our previous study for the experimental determination of threshold T_2 cut-offs (T_{2c}), from laboratory NMR experiments on shale samples brine-saturated (S_w=100%) and at irreducible saturation level ($S_{w,irr}$ measured after centrifugation and oven-drying procedures). Figure modified from Testamanti & Rezaee (2017).

and porosity values originally reported in Testamanti & Rezaee (2017) were obtained. In addition, the raw NMR data from the brine-saturated shale samples were inverted with the BRD, UPEN and NNLS-LH/GCV algorithms. The BRD inversions were also performed in Prospa, using the *Asym* option in the *Lexus* module, which approximates the regularization weights based on the asymptotic analysis of the noise (P. Aptaker, personal communication, October 2017). Moreover, the UPEN and NNLS-LH/GCV algorithms were implemented in MATLAB (MathWorks). Prior to inversion, the raw T_2 data sizes were reduced by the SVD method.

Fig. 7 shows the inverted T_2 data from the brine-saturated shale core plugs, obtained by the BRD, UPEN and NNLS-LH/GCV methods, and compared with the T_2 distributions included in the original study (labeled *NNLS-LH/L-curve*). It can be seen from the graph that these last three methods produce similarly shaped T_2 curves, where one broad peak is displayed below 3 ms. In contrast, an additional peak seems to emerge in some of the distributions obtained by the BRD inversion at short T_2 relaxation times.

The results obtained by BRD and NNLS-LH/L-curve inversions, from brine-saturated shale core plugs, are reproduced again in Fig. 8 for clarification purposes, along with the T_2 distributions from oven-dried samples (seen in dotted gray lines). While one broad peak can be observed at early times in the original T_2 spectra (NNLS-LH) from experiments

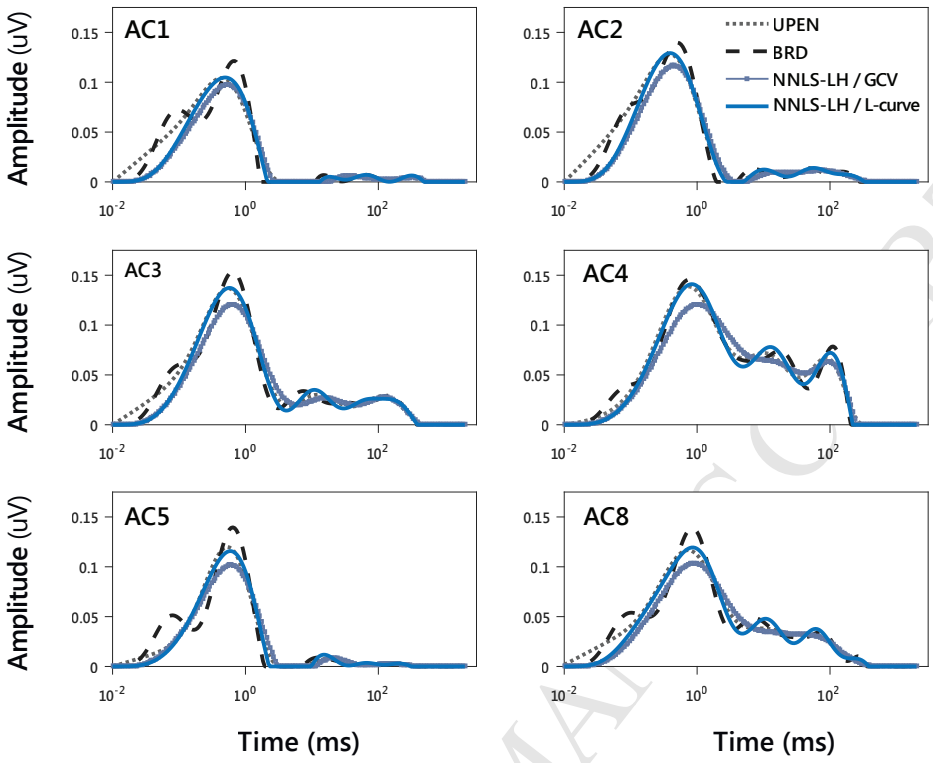

Figure 7: T_2 spectra for experimental decays from saturated shale core samples, obtained by the NNLS-LH/GCV, NNLS-LH/L-curve, BRD and UPEN methods.

in saturated shale core plugs, multiple peaks appear on the BRD inversion results. When comparing these two curves to the spectra from oven-dried samples, the main peak in the T_2 distribution corresponding to the NNLS-LH method can be reinterpreted as the overlapped response of at least two individual features, which emerge on the T_2 curve obtained by the BRD inversion. A portion of the fastest peak in the BRD inverted curves fall below the detection limit of the spectrometer used, however, they may still represent the real NMR signals which are partially detected during T_2 measurements. The signal close to and below 0.1 ms has been associated with the transverse relaxation of structural hydroxyls in clays (Fleury et al., 2013; Washburn & Birdwell, 2013) and protons in solid organic matter (Washburn, 2014). Despite the uncertainty in the real amplitude and exact location of the additional peak distinguished by the BRD inversion around 0.1 ms, the feature is indeed consistent with the NMR response expected in shales. Furthermore, two

threshold $T_{2\ \text{cut-off}}$ could be identified from the contrast of NNLH-LH and BRD inverted T_2 distributions (Fig. 8), which are also consistent with the thresholds T_{2L}, T_{2U} determined experimentally in our previous study (Testamanti & Rezaee, 2017).

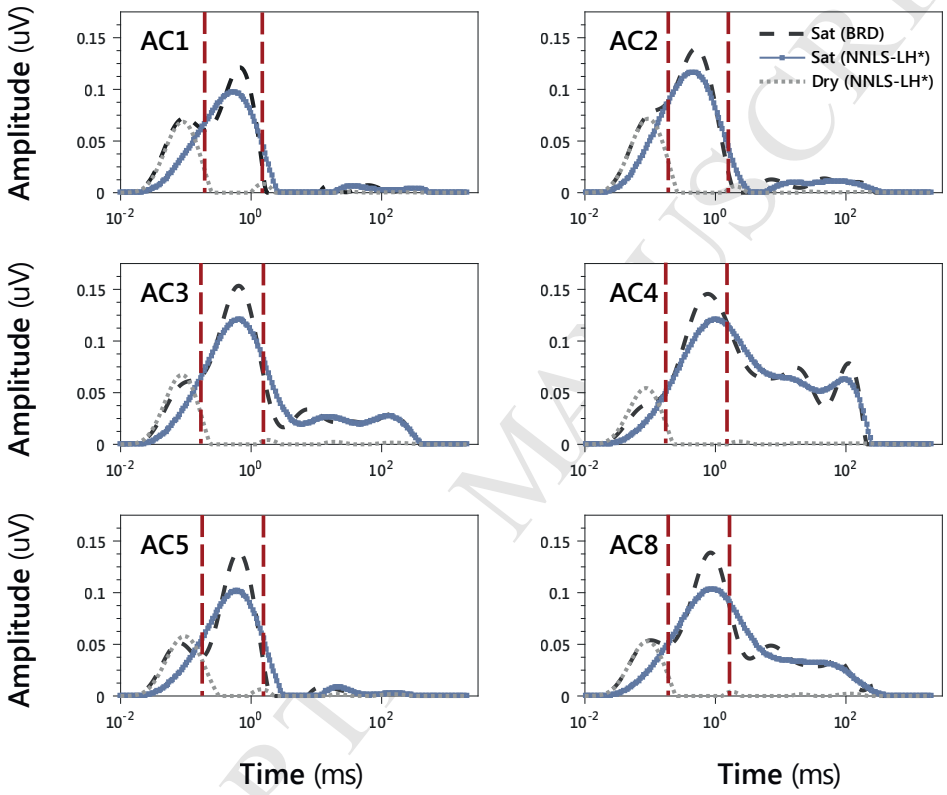

Figure 8: T_2 spectra from experimental decays on brine-saturated and oven-dried core samples, obtained by the NNLS-LH and BRD methods. The red dashed lines indicate the approximate locations of the threshold T_2 cut-offs determined analytically, from the contrast of brine-saturated T_2 distributions obtained by the different inversion methods.

5. Conclusion

In this paper, various aspects of the nuclear magnetic resonance (NMR) technique have been examined, with a focus on one-dimensional transverse relaxation (T_2) experiments for shale applications. The main findings of this research can be summarized as:

- Good quality laboratory NMR data can be difficult to obtain in shales. Increasing the number of scans could lead to improvements in the experimental SNR, but may also extend the duration of T_2 tests considerably. Alternatively, the SNR may be enhanced with the acquisition of a large number of data points, many of which will contain only noise. A good balance between noise and sensitivity to short T_2 components is therefore essential.

- The fast relaxation rates in shales pose unique challenges for the inversion of NMR data. Direct inversion approaches (e.g. NNLS-LH/L-curve) may produce very smooth T_2 distributions and lead to the potential loss of valuable qualitative information. Methods targeting noise level (e.g. BRD) may improve the quality of T_2 data inversion in shales, but may also bias the results.

- The shape of the T_2 distributions at short times were found to be greatly influenced by the choice of inversion algorithm, highlighting the importance of choosing a method that can yield results which are representative of the real T_2 relaxation mechanisms in shales.

- The threshold T_2 cut-offs determined experimentally in our previous work are consistent with values herein identified, based on the comparison of T_2 spectra obtained by forward and indirect inversion approaches. Overall, the present findings suggest that this analytical methodology could be feasibly used to estimate $T_{2\ \text{cut-off}}$ parameters in shales. Research into the petrophysical applications of these threshold $T_{2\ \text{cut-off}}$ is currently underway.

Acknowledgements

This study was supported by an Australian Government Research Training Program (RTP) Scholarship and a Curtin Research Scholarship (CRS). The authors wish to thank Mr. Andrew Lockwood (Principal Geophysicist at Woodside Energy) for his insightful comments on an early version of this manuscript. We would also like to gratefully acknowledge the JPSE Editor-in-Chief Dr. Vural Sander Suicmez and anonymous reviewers for their constructive suggestions.

Acronyms

BRD Butler-Reeds-Dawson Algorithm.

CBW Clay Bound Water.

CPMG Carr-Purcell-Meiboom-Gill.

FID Free Induction Decay.

GCV Generalised Cross-Validation Algorithm.

LH Lawson-Hanson Algorithm.

NMR Nuclear Magnetic Resonance.

NNLS Nonnegative Least Squares Method.

PSNR Peak Signal-to-Noise Ratio.

RF Radio Frequency.

RMSE Root Mean Squared Error.

SAE Sum of Absolute Error.

SNR Signal-to-Noise Ratio.

SSI Structural Similarity Index.

SVD Singular Value Decomposition.

UPEN Uniform Penalty Algorithm.

Symbols

B_0 Static Magnetic Field.

D Molecular Self-diffusion Coefficient.

γ Gyromagnetic Ratio of Precessing Nuclei.

G Magnetic Field Gradient.

λ Regularization Parameter.

$M(t)$ Proton Magnetization as a Function of Time.

M_0 Proton Magnetization at Time Zero.

N_E Number of Echoes.

ρ Surface Relaxivity.

S/V Pore Surface Area to Volume.

T_1 Longitudinal Relaxation.

T_2 Transverse Relaxation.

$T_{2\mathbf{b}}$ Transverse Relaxation of bulk fluid.

T_{acq} Total Acquisition Time.

T_E Echo Spacing.

T_W Wait Time.

References

Anovitz, L. M., & Cole, D. R. (2015). Characterization and Analysis of Porosity and Pore Structures. *Reviews in Mineralogy and Geochemistry*, *80*, 61–164. URL: http://rimg.geoscienceworld.org/content/80/1/61.short. doi:10.2138/rmg.2015.80.04.

Bloembergen, N., Purcell, E. M., & Pound, R. V. (1948). Relaxation effects in nuclear magnetic resonance absorption. *Physical Review*, *73*, 679–712. URL: https://link.aps.org/doi/10.1103/PhysRev.73.679. doi:10.1103/PhysRev.73.679.

Borgia, G. C., Brown, R. J., & Fantazzini, P. (1998). Uniform-Penalty Inversion of Multiexponential Decay Data. *Journal of Magnetic Resonance*, *132*, 65–77. doi:10.1006/jmre.1998.1387.

Borgia, G. C., Brown, R. J. S., & Fantazzini, P. (2000). Uniform-Penalty Inversion of Multiexponential Decay Data. *Journal of Magnetic Resonance*, *147*, 273–285. doi:10.1006/jmre.2000.2197.

Borgia, G. C., Fantazzini, P., & Mesini, E. (1990). Water 1H spin-lattice relaxation as a fingerprint of porous media. *Magnetic Resonance Imaging*, *8*, 435–447. doi:10.1016/0730-725X(90)90052-4.

Butler, J. P., Reeds, J. A., & Dawson, S. V. (1981). Estimating Solutions of First Kind Integral Equations with Nonnegative Constraints and Optimal Smoothing. *SIAM Journal on Numerical Analysis*, *18*, 381–397. doi:10.1137/0718025.

Chen, S., Arro, R., Minetto, C., Georgi, D., & Liu, C. (1998). Methods For Computing Swi And BVI From NMR Logs. In *SPWLA 39th Annual Logging Symposium*. Keystone, Colorado: Society of Petrophysicists and Well-Log Analysts.

Coates, G. R., Galford, J., Mardon, D., & Marschall, D. (1998). A New Characterization Of Bulk-volume Irreducible Using Magnetic Resonance. *The Log Analyst*, *39*.

Coates, G. R., Xiao, L., & Prammer, M. G. (1999). *NMR logging: principles and applications*. Houston: Halliburton Energy Services. URL: http://www.halliburton.com/public/lp/contents/Books_and_Catalogs/web/NMR-Logging-Principles-and-Applications.pdf.

Does, M. (2014). Multi-Exponential Relaxation Analysis (MERA) Toolbox. URL: http://www.vuiis.vanderbilt.edu/{~}doesmd/MERA/MERA{_}Toolbox.html.

Dunn, K. J., Bergman, D. J., & Latorraca, G. A. (2002). NMR in Porous Media.

Dunn, K.-J., LaTorraca, G. A., Warner, J. L., & Bergman, D. J. (1994). On the Calculation and Interpretation of NMR Relaxation Time Distributions. doi:10.2118/28367-MS.

Eveleigh, L. J. (1996). Fourier transform and signal manipulation. In D. N. Rutledge (Ed.), *Signal Treatment and Signal Analysis in NMR* chapter 1. (pp. 1–24). Elsevier volume Vol. 18, Data Handling in Science and Technology. doi:10.1016/S0922-3487(96)80038-4.

Fleury, M., Kohler, E., Norrant, F., Gautier, S., M'Hamdi, J., & Barré, L. (2013). Characterization and Quantification of Water in Smectites with Low-Field NMR. *The Journal of Physical Chemistry C*, *117*, 4551–4560. doi:10.1021/jp311006q.

Fordham, E. J., Sezginer, A., & Hall, L. D. (1995). Imaging Multiexponential Relaxation in the (y, LogeT1) Plane, with Application to Clay Filtration in Rock Cores. *Journal of Magnetic Resonance, Series A*, *113*, 139–150. doi:10.1006/jmra.1995.1073.

Freedman, R. (2002). Processing NMR data in the presence of coherent ringing. URL: https://patents.google.com/patent/US6838875B2/en.

Gerothanassis, I. P. (1987). Methods of avoiding the effects of acoustic ringing in pulsed fourier transform nuclear magnetic resonance spectroscopy. *Progress in Nuclear Magnetic Resonance Spectroscopy*, *19*, 267–329. doi:10.1016/0079-6565(87)80005-5.

Golub, G. H., Heath, M., & Wahba, G. (1979). Generalized Cross-Validation as a Method for Choosing a Good Ridge Parameter. *Technometrics*, *21*, 215–223. doi:10.2307/1268518.

Grebenkov, D. S. (2007). NMR survey of reflected Brownian motion. *Reviews of Modern Physics*, *79*, 1077–1137. doi:10.1103/RevModPhys.79.1077.

Hansen, P. C. (1987). The truncated SVD as a method for regularization. *BIT Numerical Mathematics*, *27*, 534–553. doi:10.1007/BF01937276.

Hansen, P. C. (1992). Numerical tools for analysis and solution of Fredholm integral equations of the first kind. *Inverse Problems*, *8*, 849. URL: http://stacks.iop.org/0266-5611/8/i=6/a=005.

Hansen, P. C. (2015). Regularization Tools for Matlab. URL: http://www.imm.dtu.dk/{~}pcha/Regutools/.

Hansen, P. C., Jensen, T. K., & Rodriguez, G. (2007). An adaptive pruning algorithm for the discrete L-curve criterion. *Journal of Computational and Applied Mathematics*, *198*, 483–492. doi:10.1016/j.cam.2005.09.026.

Hansen, P. C., & O'Leary, D. (1993). The Use of the L-Curve in the Regularization of Discrete Ill-Posed Problems. *SIAM Journal on Scientific Computing*, *14*, 1487–1503. doi:10.1137/0914086.

Hürlimann, M. D. (1998). Effective Gradients in Porous Media Due to Susceptibility Differences. *Journal of Magnetic Resonance*, *131*, 232–240. doi:10.1006/jmre.1998.1364.

Hürlimann, M. D., & Venkataramanan, L. (2002). Quantitative Measurement of Two-Dimensional Distribution Functions of Diffusion and Relaxation in Grossly Inhomogeneous Fields. *Journal of Magnetic Resonance*, *157*, 31–42. doi:10.1006/jmre.2002.2567.

Kenyon, W. E. (1997). Petrophysical Principles of Applications of NMR Logging. *The Log Analyst*, *38*, 21–43.

Kleinberg, R. L. (1999). 9. Nuclear Magnetic Resonance. In P.-z. B. T. E. M. i. t. P. S. Wong (Ed.), *Methods in the Physics of Porous Media* (pp. 337–385). Academic Press volume 35. doi:10.1016/S0076-695X(08)60420-2.

Kleinberg, R. L., Straley, C., Kenyon, W. E., Akkurt, R., & Farooqui, S. A. (1993). Nuclear Magnetic Resonance of Rocks: T1 vs. T2. In *SPE Annual Technical Conference and Exhibition*. Houston, Texas, USA: Society of Petroleum Engineers. doi:10.2118/26470-MS.

Lawson, C. L., & Hanson, R. J. (1974). 26. Examples of Some Methods of Analyzing a Least Squares Problem. In *Solving Least Squares Problems* chapter 26. (pp. 199–206). doi:10.1137/1.9781611971217.ch26.

McPhee, C., Reed, J., & Zubizarreta, I. (2015). Chapter 11 - Nuclear Magnetic Resonance (NMR). In J. R. Colin McPhee, & Z. Izaskun (Eds.), *Developments in Petroleum Science* (pp. 655–669). Elsevier volume Volume 64. doi:10.1016/B978-0-444-63533-4.00011-1.

Miao, J., Huo, D., & Wilson, D. L. (2008). Quantitative image quality evaluation of MR images using perceptual difference models. *Medical Physics*, *35*, 2541–2553. doi:10.1118/1.2903207.

Mitchell, J., Chandrasekera, T. C., & Gladden, L. F. (2012). Numerical estimation of relaxation and diffusion distributions in two dimensions. *Progress in Nuclear Magnetic Resonance Spectroscopy*, *62*, 34–50. doi:10.1016/j.pnmrs.2011.07.002.

Moody, J. B., & Xia, Y. (2004). Analysis of multi-exponential relaxation data with very short components using linear regularization. *Journal of Magnetic Resonance*, *167*, 36–41. doi:10.1016/j.jmr.2003.11.004.

Morozov, V. A. (1984). *Methods for Solving Incorrectly Posed Problems*. New York: Springer.

Mory, A., & Iasky, R. (1996). *Stratigraphy and structure of the onshore northern Perth Basin, Western Australia*. Technical Report Western Australia: Western Australia Geological Survey.

Pearce, C. E. M., Abbott, D., McDonnell, M. D., & Stocks, N. G. (2008). Stochastic resonance: its definition, history, and debates. In *Stochastic Resonance: From Suprathreshold Stochastic Resonance to Stochastic Signal Quantization* chapter 2. (pp. 6–46). Cambridge: Cambridge University Press. doi:10.1017/CBO9780511535239.004.

Polyanin, A. D., & Manzhirov, A. V. (2008). *Handbook of Integral Equations: Second Edition*. Handbooks of Mathematical Equations (2nd ed.). CRC Press.

Prammer, M. G. (1994). NMR Pore Size Distributions and Permeability at the Well Site. doi:10.2118/28368-MS.

Prammer, M. G., Drack, E. D., Bouton, J. C., & Gardner, J. S. (1996). Measurements of Clay-Bound Water and Total Porosity by Magnetic Resonance Logging. *Log Analyst*, *37*, 61–69. doi:10.2118/36522-MS.

Rutledge, D. N. (1996). *Signal Treatment and Signal Analysis in NMR* volume 18. (1st ed.). Elsevier Science.

Saidian, M. (2015). *Effect of rock composition and texture on pore size distributions in shales: Applications in low field nuclear magnetic resonance*. Ph.D. thesis Colorado School of Mines.

Salimifard, B., Dick, M., Green, D., & Ruth, D. W. (2017). Optimizing NMR Data Acquisition and Data Processing Parameters for Tight-Gas Montney Formation of Western Canada. In *International Symposium of the Society of Core Analysts*. Vienna, Austria: Society of Core Analysts.

Song, Y. Q. (2000). Determining Pore Sizes Using an Internal Magnetic Field. *Journal of Magnetic Resonance*, *143*, 397–401. doi:10.1006/jmre.1999.2012.

Song, Y. Q. (2003). Using internal magnetic fields to obtain pore size distributions of porous media. *Concepts in Magnetic Resonance Part A*, *18A*, 97–110. doi:10.1002/cmr.a.10072.

Song, Y. Q., Venkataramanan, L., & Burcaw, L. (2005). Determining the resolution of Laplace inversion spectrum. *The Journal of Chemical Physics*, *122*, 104104. doi:10.1063/1.1858436.

Song, Y. Q., Venkataramanan, L., Hürlimann, M. D., Flaum, M., Frulla, P., & Straley, C. (2002). T1T2 Correlation Spectra Obtained Using a Fast Two-Dimensional Laplace Inversion. *Journal of Magnetic Resonance*, *154*, 261–268. doi:10.1006/jmre.2001.2474.

Sun, B., & Dunn, K.-J. (2004). Methods and limitations of NMR data inversion for fluid typing. *Journal of Magnetic Resonance*, *169*, 118–128. URL: http://www.sciencedirect.com/science/article/pii/S1090780704001028. doi:10.1016/j.jmr.2004.04.009.

Testamanti, M. N., & Rezaee, R. (2017). Determination of NMR T_2 cut-off for clay bound water in shales: A case study of Carynginia Formation, Perth Basin, Western Australia. *Journal of Petroleum Science and Engineering*, *149*, 497–503. doi:10.1016/j.petrol.2016.10.066.

Tikhonov, A. N. (1963). Solution of Incorrectly Formulated Problems and the Regularization Method. *Soviet Math. Dokl.*, *5*, 1035–1038. URL: http://ci.nii.ac.jp/naid/10004315593/en/.

Twomey, S. (1963). On the Numerical Solution of Fredholm Integral Equations of the First Kind by the Inversion of the Linear System Produced by Quadrature. *Journal of the ACM*, *10*, 97–101. doi:10.1145/321150.321157.

Venkataramanan, L., Gruber, F. K., Habashy, T. M., Akkurt, R., Vissapragada, B., Lewis, R. E., & Rylander, E. (2013). Methods of investigating formation samples using NMR data. URL: https://patents.google.com/patent/US9939506B2/en.

Venkataramanan, L., Song, Y. Q., & Hürlimann, M. D. (2002). Solving Fredholm integrals of the first kind with tensor product structure in 2 and 2.5 dimensions. *IEEE Transactions on Signal Processing*, *50*, 1017–1026. doi:10.1109/78.995059.

Wang, Z., Bovik, A. C., Sheikh, H. R., & Simoncelli, E. P. (2004). Image quality assessment: from error visibility to structural similarity. *IEEE Transactions on Image Processing*, *13*, 600–612. doi:10.1109/TIP.2003.819861.

Washburn, K. (2014). Relaxation mechanisms and shales. *Concepts in Magnetic Resonance Part A*, *43A*, 57–78. doi:10.1002/cmr.a.21302.

Washburn, K., Anderssen, E., Vogt, S., Seymour, J. D., Birdwell, J. E., Kirkland, C. M., & Codd, S. L. (2015). Simultaneous Gaussian and exponential inversion for improved analysis of shales by NMR relaxometry. *Journal of Magnetic Resonance*, *250*, 7–16. doi:10.1016/j.jmr.2014.10.015.

Washburn, K., & Birdwell, J. (2013). Updated methodology for nuclear magnetic resonance characterization of shales. *Journal of Magnetic Resonance*, *233*, 17–28. doi:10.1016/j.jmr.2013.04.014.

Watson, A. T., & Chang, C. T. P. (1997). Characterizing porous media with NMR methods. *Progress in Nuclear Magnetic Resonance Spectroscopy*, *31*, 343–386. doi:10.1016/S0079-6565(97)00053-8.

Whittall, K. P. (1994). Analysis of Large One-Dimensional and Two-Dimensional Relaxation Data Sets. *Journal of Magnetic Resonance, Series A*, *110*, 214–218. doi:10.1006/jmra.1994.1207.

Whittall, K. P. (1996). Analysis of NMR Relaxation Data. In D. N. Rutledge (Ed.), *Signal Treatment and Signal Analysis in NMR* chapter 3. (pp. 44–67). Elsevier volume Vol. 18, Data Handling in Science and Technology. doi:10.1016/S0922-3487(96)80040-2.

Highlights

- Evaluation of critical parameters in NMR T_2 data acquisition and processing for shale applications
- Sensitivity analysis to various signal acquisition parameters from *T2* experiments in shale cores
- Short echo spacings (*TE*) can improve signal quality but also enhance early experimental noise
- Inversion methods using fixed smoothing cannot resolve adjacent *T2* components correctly
- Inversion methods based on noise level produce better fits but may bias solutions
- The *BRD* algorithm can differentiate the contribution from adjacent peaks at short *T2* times
- Threshold T_2 cut-offs are determined analytically by using two different NMR inversion methods